



**HAL**  
open science

## Self-healing polyacrylate coatings with dynamic H-bonds between urea groups

Marie Mottoul, Sylvain Giljean, Marie-josé Pac, Véronic Landry, Jean-françois  
Morin

► **To cite this version:**

Marie Mottoul, Sylvain Giljean, Marie-josé Pac, Véronic Landry, Jean-françois Morin. Self-healing polyacrylate coatings with dynamic H-bonds between urea groups. *Journal of Applied Polymer Science*, 2023, 10.1002/app.53853 . hal-04048154

**HAL Id: hal-04048154**

**<https://hal.science/hal-04048154v1>**

Submitted on 27 Mar 2023

**HAL** is a multi-disciplinary open access archive for the deposit and dissemination of scientific research documents, whether they are published or not. The documents may come from teaching and research institutions in France or abroad, or from public or private research centers.

L'archive ouverte pluridisciplinaire **HAL**, est destinée au dépôt et à la diffusion de documents scientifiques de niveau recherche, publiés ou non, émanant des établissements d'enseignement et de recherche français ou étrangers, des laboratoires publics ou privés.

# Self-Healing Polyacrylate Coatings with Dynamic H-Bonds Between Urea Groups

Marie Mottoul,<sup>†,‡</sup> Sylvain Giljean,<sup>¶</sup> Marie-José Pac,<sup>¶</sup> Véronic Landry,<sup>‡</sup> and Jean-François Morin<sup>\*,†</sup>

<sup>†</sup>*Département de chimie and Centre de Recherche sur les Matériaux Avancés (CERMA),  
1045 Ave de la Médecine, Université Laval, Québec, Canada G1V 0A6*

<sup>‡</sup>*Canlak Industrial Research Chair in Interior Wood Product Finishes, Département des sciences du bois et de la forêt, 2425 rue de la Terrasse, Université Laval, Québec, Canada  
G1V 0A6*

<sup>¶</sup>*Université de Haute-Alsace, Laboratoire de Physique et Mécanique Textiles (UR 4365),  
68093 Mulhouse, France*

E-mail: jean-francois.morin@chm.ulaval.ca

## Abstract

Adding self-healing properties to coatings is a promising way to increase their lifetime. Despite an increasing popularity, lots of self-healing polymers are not suited for commercial coatings because they exhibit poor mechanical properties or require expensive products or high healing temperature ( $> 100$  °C). One way to obtain self-healing abilities with good mechanical properties is by using dynamic H-bonds as they also limit the healing temperature. To do so, urea groups are used since they are well-known for their bonding capacity and can be readily synthesized. In this study, several methacrylate monomers containing urea groups in their side-chain were synthesized from easily accessible amines and isocyanates in a

one-step, high-yield synthesis. They were afterwards used in a copolymer containing methyl methacrylate and butyl acrylate monomers. The self-healing properties of the resulting coatings were evaluated with gloss recovery and optical microscopy and the presence of H-bonds in the most promising polymer was investigated with FTIR. The mechanical properties of the coatings as a function of time were checked by nanoindentation creep test. We were able to obtain an affordable, easily prepared polymer that suits the requirements for protective coating applications and shows a complete healing after heating at 75 °C for 1 h.

## Introduction

Self-healing materials have attracted attention due to their ability to recover their functions and properties after damage, thus allowing the development of materials with an extended lifetime. In particular, self-healing properties are beneficial to coatings since their main function is to protect the substrate from mechanical aggression, putting them at risk to be damaged. Self-healing behavior can be accessed through extrinsic or intrinsic approaches. The former approach usually requires capsules containing liquid healing reagent such as monomers<sup>1-3</sup>. Under stress, the capsules break, releasing the fluid which will flow inside the crack and polymerize under the appropriate conditions. This process is autonomous but cannot be repeated and, consequently, does not suit surfaces used on a daily basis, with mechanical damages occurring at the same place.

The key to obtain a repeatable repair is an intrinsic approach, usually based on dynamic interactions. Many strategies have been developed using reversible covalent bonds<sup>4-10</sup>, H-bonds<sup>11-14</sup>, coordination bonds<sup>15,16</sup>,  $\pi - \pi$  interactions<sup>17</sup>, host-guest interactions<sup>18,19</sup> and ionic interactions<sup>20-22</sup>. Although van der Waals interactions were demonstrated as being part of the self-healing process<sup>23</sup>, their role is still poorly reported in the literature. In addition to reversible interactions, chain mobility is a major feature to consider in order to

access intrinsic healing. Wool and O'Connor<sup>24</sup> highlighted its importance by depicting the self-healing phenomenon as a five-step process occurring after damage: a) surface rearrangements and b) surface approach, c) wetting of the damaged surfaces by each other allowing the d) diffusion of the polymer chains from both sides of the damage, which results in entanglements and eventually e) randomization, involving loss of memory of the damaged surface if the healing is complete. Chain mobility can easily be achieved with soft polymers but induces poor mechanical performances. Depending on the targeted application, more robust polymers and consequently higher glass transition temperatures ( $T_g$ ) may be required and it is then necessary to heat above the  $T_g$  to favor the movements of the polymer chains.

One of the most popular approaches to use reversible covalent bonds in a polymer involves the Diels-Alder (DA) reaction between furan and maleimide moieties, forming a DA adduct that is either part of the polymer backbone<sup>25</sup> or acting as cross-linker in side chains<sup>26</sup>. The dissociation of the adduct through a retro-Diels-Alder reaction takes place over 110 °C and allows a rearrangement of the polymer chains, triggering the healing process. However, this temperature may be excessive for temperature-sensitive substrates such as wood. H-bonds are then a good alternative for the design of a self-healing polymer. After being broken by mechanical aggression, they can be restored owing to their dynamic nature. Although they are individually weak, they are collectively strong and endow the polymer with good mechanical properties through the formation of a dynamic non-covalent cross-linked network, decreasing the self-healing temperature compared to DA reaction.

Polyacrylates and their derivatives are well-known commodity polymers in the coating industry. They are low-cost, transparent, versatile and exhibit good mechanical behavior. Nevertheless, only a few articles have been reported for their use as self-healing materials. Wouters *et al.* were the first to use the DA healing strategy on polymethacrylate polymers through the use of a furfuryl methacrylate monomer and a bis-maleimide cross-

linking reagent<sup>27</sup>. In 2013, the group of Prof. Schubert studied the reversible cross-linking of one-component polymethacrylates while including both furan and maleimide as pendant groups<sup>28,29</sup>. In another work, they adapted the DA strategy with anthracene units and fullerenes as dienes and dienophiles<sup>26</sup>. More recently, Schäfer *et al.* designed a hybrid polymethacrylate network bearing both DA moieties in addition to ureas and amides interacting with spherosilicates through H-bonds<sup>30</sup>. Urban *et al.* showed that statistical copolymers made from methyl methacrylate (MMA) and *n*-butyl acrylate (BuA) are able to recover from a 20  $\mu\text{m}$  scratch under ambient conditions owing to van der Waals interactions occurring between the butyl chains<sup>23</sup>. Butyl acrylate-based copolymers were synthesized with 2-ureido-4[1H]-pyrimidinone groups embedded in the side chains<sup>12</sup>. This unit is able to form a dimer through quadrupole-H-bonding and then brings self-healing properties to the material. In 2020, Wu *et al.* reported the preparation of a waterborne photoluminescent polyacrylate coating whose self-healing properties are brought by ionic interactions and H-bonds<sup>31</sup>. Nevertheless, the healing process is triggered by immersion of the sample in water, which can be a major drawback for future applications.

In this work, the self-healing properties of polyacrylate coatings containing urea groups are studied for wood coating applications. Their H-bonding capacities are well-known in supramolecular chemistry<sup>32-34</sup> and biology as they play a central role in the functions of proteins and nucleic acids<sup>35</sup>, NH H-donors interacting with the carbonyl group of a neighboring urea group (**Figure 1**). Most of the methacrylate-urea (MU) monomers can be synthesized from a methacrylate-isocyanate (MI) monomer and an amine in a one-step, high-yield synthesis. Different combinations of those two units allow tuning the monomer structure and the number of H-bond donors, impacting the self-healing properties and mechanical properties of the final coating. Owing to the simplicity of the synthesis and the easy access of the starting materials, these coatings will be particularly suited for an industrial application on wood products, or other temperature-sensitive substrates. As coatings are

more likely to be damaged with scratches, the scratch recovery properties are reported for the synthesized polymers. The presence of H-bonds were studied with FTIR spectroscopy and the mechanical properties of the coatings were assessed with creep nanoindentation tests.

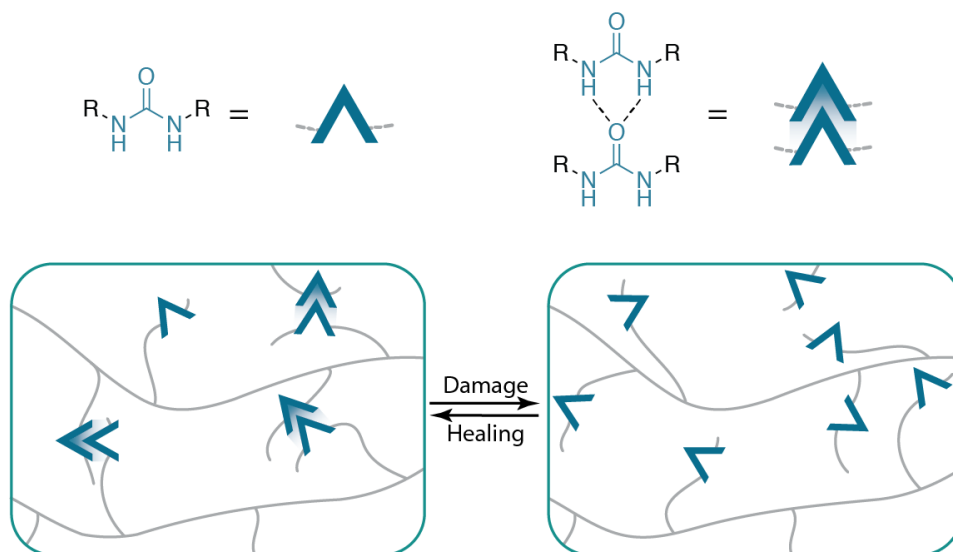


Figure 1: Formation and cleavage of H-bonds between urea moieties, allowing self-healing.

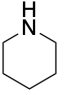
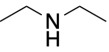

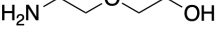
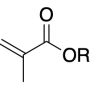

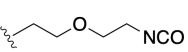
## Results and discussion

### Preparation of the polymers

As part of this study, H-bonds are embedded through urea groups in a polyacrylate copolymer based on MMA and BuA. In order to obtain several urea structures, four amines were selected to react with two different MI molecules, allowing the formation of eight different MU comonomers (**Table 1**, **Scheme 1**). The difference between the two MI molecules lies in the nature of the linker located between the methacrylate part and the isocyanate, which is either an ethyl or ethoxyethyl chain, forming PA<sub>1</sub> or PA<sub>2</sub>-type polyacrylates. The ethoxyethyl chain being longer and more flexible compared to the ethyl, a higher mobility of the urea group and then a more efficient self-healing are expected. Regarding the

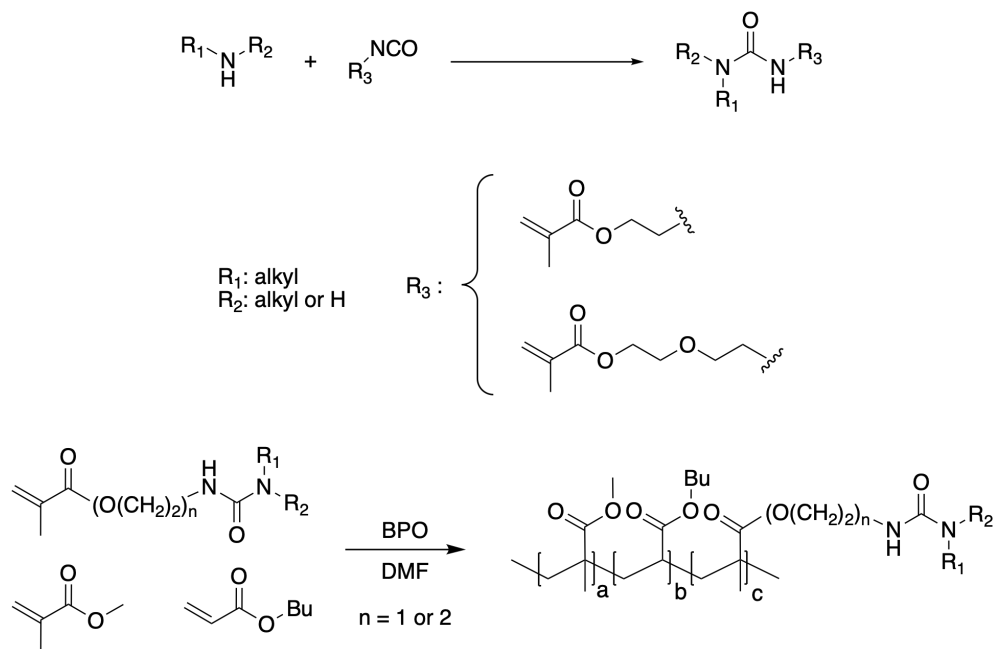
amines, four aliphatic molecules were selected based on their availability : piperidine (Pi), diethylamine (Di), *n*-butylamine (Bu) and 2-(2-aminoethoxy)ethanol (EE). As secondary amines, piperidine and diethylamine will form an urea group with a lower H-bonding potential as only one H-bond donor will be available. On the other hand, *n*-butylamine and 2-(2-aminoethoxy)ethanol are primary amines and give rise to ureas bearing an extra donor. Moreover, 2-(2-aminoethoxy)ethanol provides an hydroxyl group acting simultaneously as an H-bond donor and acceptor. The polymer were prepared with molar ratios between MMA, BuA and the MU comonomer of 40 %, 40 % and 20 % respectively. The polymer **PA<sub>0</sub>**, without any MU comonomer, acts as a reference to judge the impact of H-bonds on self-healing and  $T_g$  and was prepared with equimolar ratios of MMA and BuA.

Table 1: Identification of the synthesized comonomers depending on the amine and the MI used for the synthesis. The corresponding copolymers are identified with a P preceding the name of the comonomer. The polymer without any MU comonomer is identified as **PA<sub>0</sub>**.

Methacrylates-isocyanates (MI)		Amines			
					
	R: 	A <sub>1</sub> -Pi	A <sub>1</sub> -Di	A <sub>1</sub> -Bu	A <sub>1</sub> -EE
		A <sub>2</sub> -Pi	A <sub>2</sub> -Di	A <sub>2</sub> -Bu	A <sub>2</sub> -EE

## FTIR spectroscopy

The polymers were analyzed using FTIR to confirm the polymerization of the MU comonomer with MMA and BuA. As an example, the spectrum of **PA<sub>1</sub>-EE** was compared to the spectrum of **PA<sub>0</sub>** (without any MU comonomer) (**Figure 2**) in order to highlight the presence of the MU. Both spectra show a characteristic C=O stretching vibration band around 1725  $\text{cm}^{-1}$ , and a C-O stretching vibration at 1130  $\text{cm}^{-1}$  due to the ester moieties.<sup>36,37</sup> C-H stretching vibration bands can also be observed between 2800  $\text{cm}^{-1}$  and 3000  $\text{cm}^{-1}$ . The spectrum of **PA<sub>1</sub>-EE** also exhibits the so-called amide I band at 1645  $\text{cm}^{-1}$ , the amide II band, mainly



Scheme 1: Formation of the methacrylate-urea comonomers from an isocyanate and an amine and polymerization.

due to N-H bending, at  $1560 \text{ cm}^{-1}$  as well as the C-N stretching band at  $1064 \text{ cm}^{-1}$ .<sup>38</sup> The large band located between  $3100 \text{ cm}^{-1}$  and  $3500 \text{ cm}^{-1}$  is assessed to the N-H and O-H stretching vibrations. Those analyses suggest that the MU monomer reacted properly during the polymerization and is part of the polymer. Similar conclusions were drawn from the spectra of other polymers, available in the Supporting Information section.

The presence of H-bonds in the **PA<sub>1</sub>-EE** polymer was investigated using temperature-dependent FTIR. The spectra were acquired from  $25 \text{ }^\circ\text{C}$  to  $100 \text{ }^\circ\text{C}$ . Under heating, the amide II band at  $1560 \text{ cm}^{-1}$ , whose main contribution is N-H bending vibration, exhibits a shift to lower wavenumbers (**Figure 3**) whereas a shift to higher wavenumbers is observed for the amide I band at  $1645 \text{ cm}^{-1}$ , mainly associated with the C=O stretching vibration of the urea groups.<sup>37</sup> The bending mode of a N-H bond involved in an H-bond is expected to shift to higher wavenumbers compared to a “free” N-H bond.<sup>39</sup> Increasing temperature however tends to disrupts H-bonds and therefore favors a shift to lower wavenumbers. At



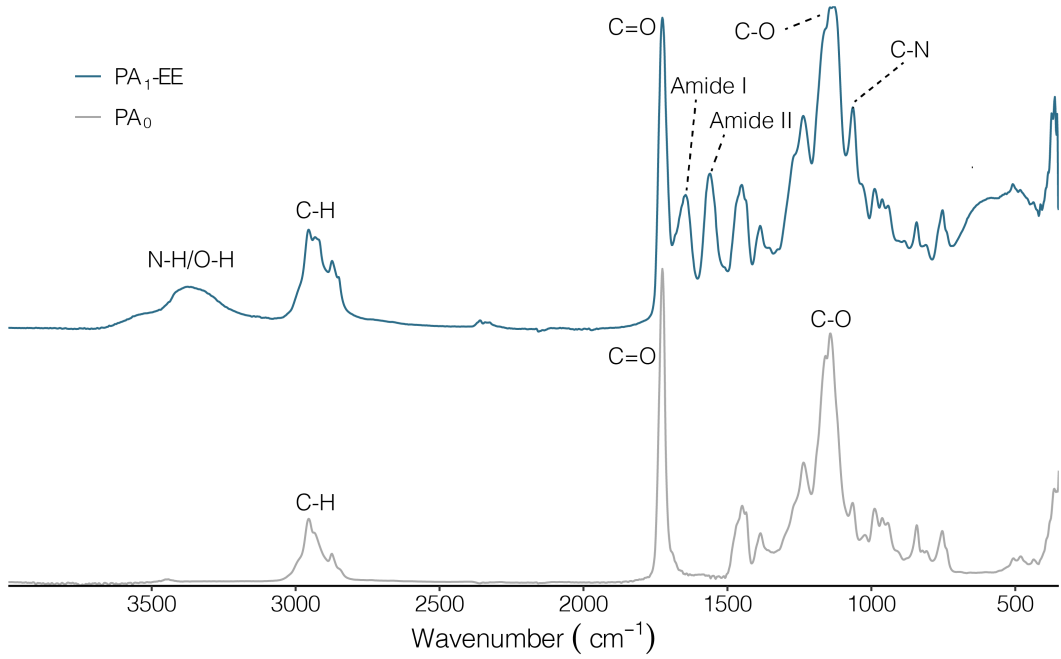


Figure 2: FTIR spectra of **PA<sub>1</sub>-EE** and **PA<sub>0</sub>**.

the opposite, C=O stretching mode is shifted to lower wavenumbers when part of a H-bond and a shift to higher wavenumbers is consequently observed under the influence of heating.<sup>39</sup> In consequence, the performed analysis strongly suggests that H-bonds are formed in the polymer.

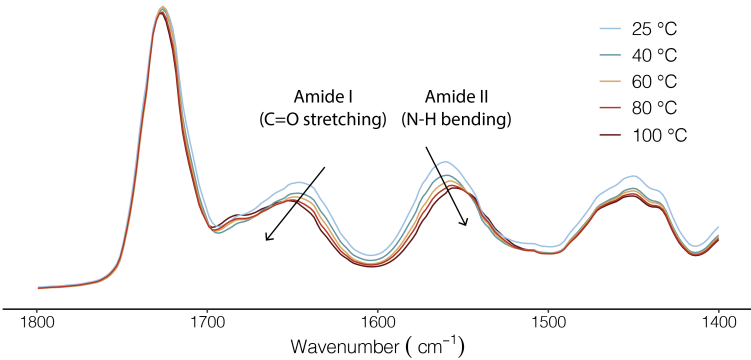


Figure 3: Zoom on the region between  $1800\text{ cm}^{-1}$  and  $1400\text{ cm}^{-1}$  of the temperature-dependant FTIR spectrum of **PA<sub>1</sub>-EE**.

## Characterization of the polymers

All the polymers were characterized using differential scanning calorimetry (DSC) and size exclusion chromatography (SEC) to obtain the  $T_g$  values and the molecular weight values of the polymers (**Table 2**). The obtained  $T_g$  range goes from 11 °C to 57 °C. The number average molecular weight ( $M_n$ ) values of the *n*-butylamine-based monomers were the highest with 143 000 g/mol and 103 300 g/mol (polydispersity indexes of 2.5 and 5.3) for **PA<sub>1</sub>-Bu** and **PA<sub>2</sub>-Bu**, respectively. The seven other polymers showed  $M_n$  values between 22 600 g/mol and 88 600 g/mol, with polydispersity indexes varying between 2.4 and 5.0.

## Self-healing properties

In order to assess their self-healing efficiency, the coatings were damaged with an abrasive pad to create scratches. The depth of the deepest scratches was measured with optical profilometry and the resulting values are available in the Supporting Information section (Table S1). Gloss recovery was chosen as a quick and efficient characterization technique to quantify the self-healing properties from gloss values (Table S1 in supporting information section). Initially, the surface of the virgin coatings is smooth and glossy. The abrasion damages create roughness at the surface, decreasing the gloss. After healing, the scratches may be filled by the polymer inducing a partial or total recovery of the gloss.

When compared to the  $T_g$  values of the PA<sub>1</sub>-based polymers, the  $T_g$  values of the PA<sub>2</sub> series are lower. This difference can be attributed to the high degree of freedom of the oxygen of the ether embedded in the lateral chain of the A<sub>2</sub>-type comonomers. In consequence, the lateral chain exhibits a higher mobility, reducing the stacking between each polymer chain and thus the rigidity of the polymeric system. Since the self-healing ability is closely related to the chain mobility, the PA<sub>2</sub> polymers tend to show better self-healing properties than the PA<sub>1</sub> series (**Figure 4**). The polymers **PA<sub>1</sub>-Pi**, **PA<sub>1</sub>-Di** and **PA<sub>1</sub>-Bu** exhibited poor

Table 2:  $T_g$  values, number average ( $M_n$ ) and weight average ( $M_w$ ) molecular weights values and polydispersity indexes ( $D$ ) of the synthesized polymers.

Polymers	$T_g$ (°C)	$M_n$ (g/mol)	$M_w$ (g/mol)	$D$
<b>PA<sub>0</sub></b>	26	24 000	64 100	2.7
<b>PA<sub>1</sub>-Pi</b>	57	81 500	406 600	5.0
<b>PA<sub>1</sub>-Di</b>	51	88 600	352 400	4.0
<b>PA<sub>1</sub>-Bu</b>	54	143 000	362 000	2.5
<b>PA<sub>1</sub>-EE</b>	39	50 800	144 700	2.9
<b>PA<sub>2</sub>-Pi</b>	30	62 200	148 000	2.4
<b>PA<sub>2</sub>-Di</b>	16	29 500	129 800	4.4
<b>PA<sub>2</sub>-Bu</b>	30	103 300	548 000	5.3
<b>PA<sub>2</sub>-EE</b>	11	22 600	100 600	4.4

self-healing due to their high  $T_g$  values. In both series, **PA<sub>1</sub>-Bu** and **PA<sub>2</sub>-Bu** showed the lowest gloss recovery. This may be due to the high molecular weight of those two polymers, hindering the diffusion step necessary to complete the self-healing mechanism.<sup>24</sup>

Amongst the tested polymers, **PA<sub>1</sub>-EE** seems to be the best option to be used as a protective coating. Even if **PA<sub>2</sub>-Di** and **PA<sub>2</sub>-EE** exhibit a 100 % gloss recovery, their  $T_g$  values are low and the resulting coatings are soft and can therefore be easily deformed. **PA<sub>2</sub>-Pi** shows a high gloss recovery value of 93%, but it has been observed that piperidine-based polymers tend to appear yellow, which can be due to a very small amount of decomposition product of this amine. This may be an issue for aesthetic reason if those polymers are applied as coatings on clear substrates. The self-healing ability of the **PA<sub>1</sub>-EE** polymer can be explained with two main factors: 1) 2-(2-aminoethoxy)ethanol confers a good H-bonding potential to the resulting MU comonomer owing to the oxygen of the ether group, the hydroxy group and the two hydrogen atoms on the urea moiety and 2) the ethoxyethanol moiety is mobile owing to the ether, favoring the reconnection of H-bonds during the self-healing process.

The positive influence of the H-bonds on the self-healing process can be highlighted by comparing **PA<sub>0</sub>** and **PA<sub>1</sub>-EE**. On one hand, **PA<sub>0</sub>** shows a weak potential for H-bonding

but its  $T_g$  value of 26 °C favors self-healing, which is clearly observed on **Figure 5a** and **5b**. However, this  $T_g$  value may be insufficient depending on the targeted application. On the other hand, **PA<sub>1</sub>-EE** exhibits a higher potential for H-bonding, has a higher  $T_g$  value and demonstrates a complete healing phenomenon (**Figure 5c** and **5d**). Since the main difference between those polymers lies in the presence of a 2-(2-aminoethoxy)ethanol-based MU comonomer in **PA<sub>1</sub>-EE** structure, the H-bonds between the chains of **PA<sub>1</sub>-EE** play a central role to obtain self-healing while providing a good  $T_g$  value at the same time.

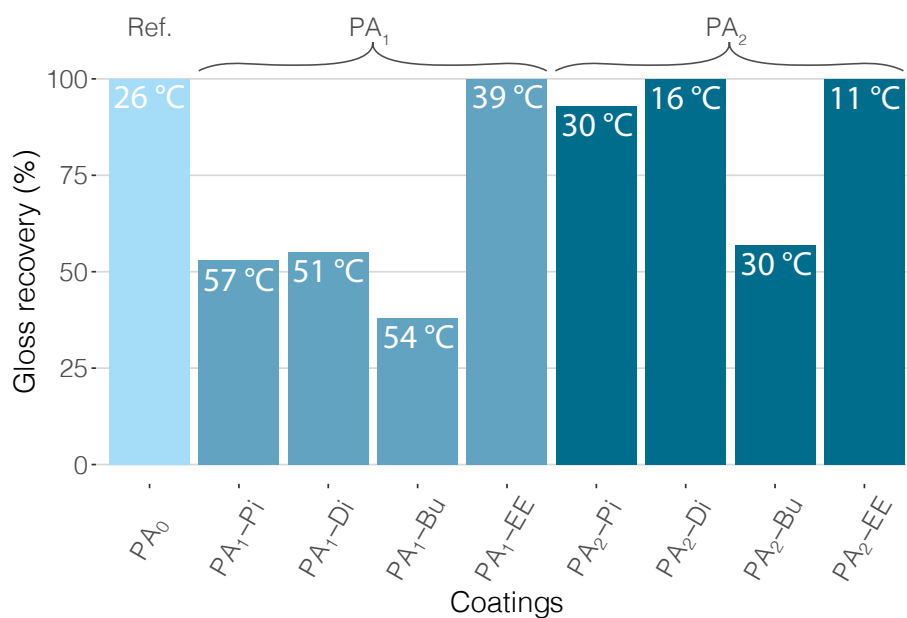


Figure 4: Gloss recovery of the damaged coatings after heating at 75 °C for 1h and their  $T_g$  values.

## Mechanical properties

The surface properties of the five coatings exhibiting a gloss recovery value higher than 90 % were investigated with nanoindentation analyses. Nanoindentation tests were carried out at room temperature with a Berkovich indenter. Scanning Probe Microscopy (SPM) images (**Figure 6**) show that the coatings exhibited visco-elastic/visco-plastic mechanical properties<sup>40</sup> as the depth of the indentation imprint significantly decreases 30 minutes after

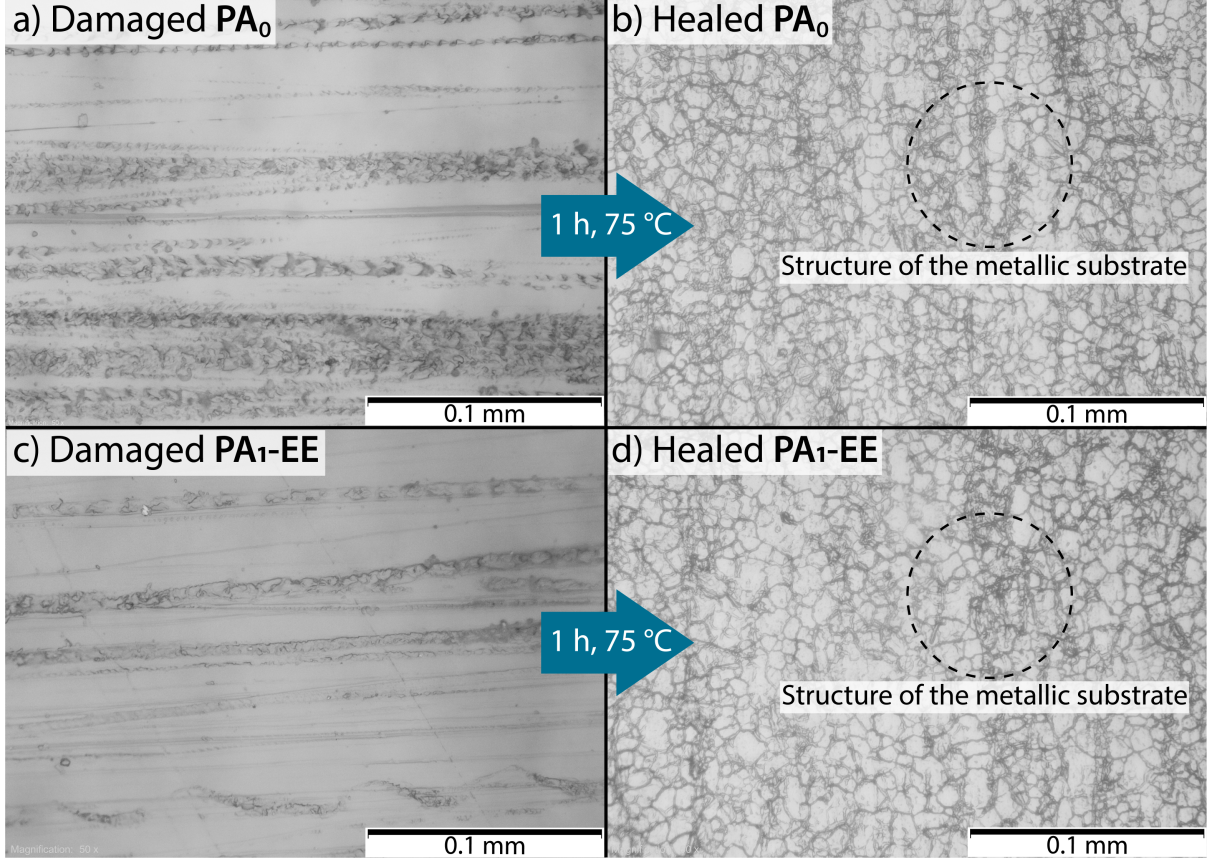


Figure 5: Optical microscopy images of  $\text{PA}_0$  and  $\text{PA}_1\text{-EE}$  after abrasion and after heating at  $75\text{ }^\circ\text{C}$  for 1h, where only the back metallic substrate can be seen.

the indentation test. Then, continuous measurements of mechanical properties during an indentation creep test were performed with a reference frequency technique for thermal drift correction during the course of experiment.

The instrumented hardness ( $H_{IT}$ ) is defined as :

$$H_{IT} = \frac{F_m}{A_c} \quad (1)$$

where  $F_m$  is the maximal applied load and  $A_c$  the projected contact area between the tip and the coating. For a perfect Berkovich indenter,  $A_c$  is equal to  $24.56 h_c^2$  with  $h_c$  being the contact depth. In practice,  $A_c$  is commonly defined by Oliver and Pharr model who

added other terms to consider tip blunting.<sup>41</sup> The mean hardness curves, determined with at least five tests on each sample, were plotted as a function of the time (**Figure 7**). During the first 10 seconds of the test, the increase of hardness is not related to the coatings but is due to the insufficient contact area between the tip and the coating that does not allow the true calculation of hardness by Oliver and Pharr method. After 10 seconds, the creep properties of the coatings induce an increase of the penetration depth and consequently a decrease of the hardness. The final hardness after 5 minutes ranged from 15 to 86 MPa for **PA<sub>2</sub>-EE** and **PA<sub>1</sub>-EE** respectively, showing that hardness is clearly linked to the  $T_g$  value. Higher  $T_g$  values were indeed obtained with higher hardnesses. Within the five coatings leading to a gloss recovery of 100 %, **PA<sub>1</sub>-EE** shows the best mechanical performance. Once more, those analyses suggest the positive role of H-bonds to obtain self-healing abilities and mechanical properties simultaneously since the hardness of **PA<sub>1</sub>-EE** is higher than the one of the reference **PA<sub>0</sub>**.

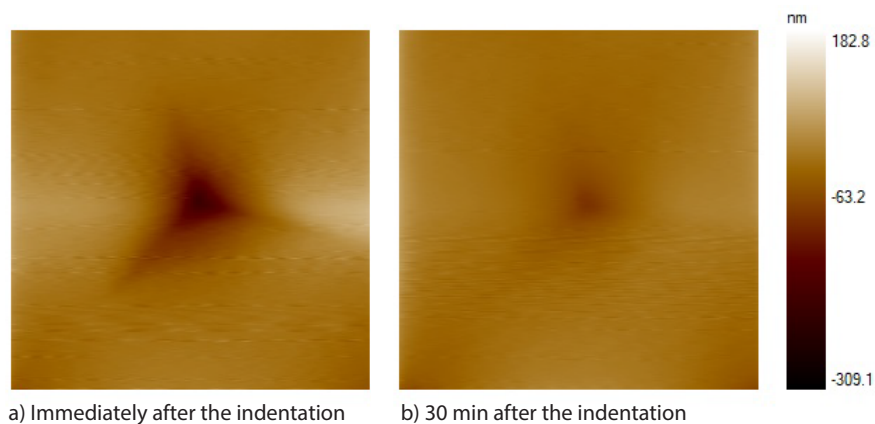


Figure 6:  $20 \times 20 \mu\text{m}^2$  Scanning Probe Microscopy images of residual indentation imprint on coating **PA<sub>2</sub>-EE** a) immediately after the indentation test and b) 30 minutes after the indentation test.

## Conclusion and outlook

In this work, self-healing polyacrylate coatings were successfully prepared by using H-bond interactions between urea groups. Several monomers synthesized from different combinations

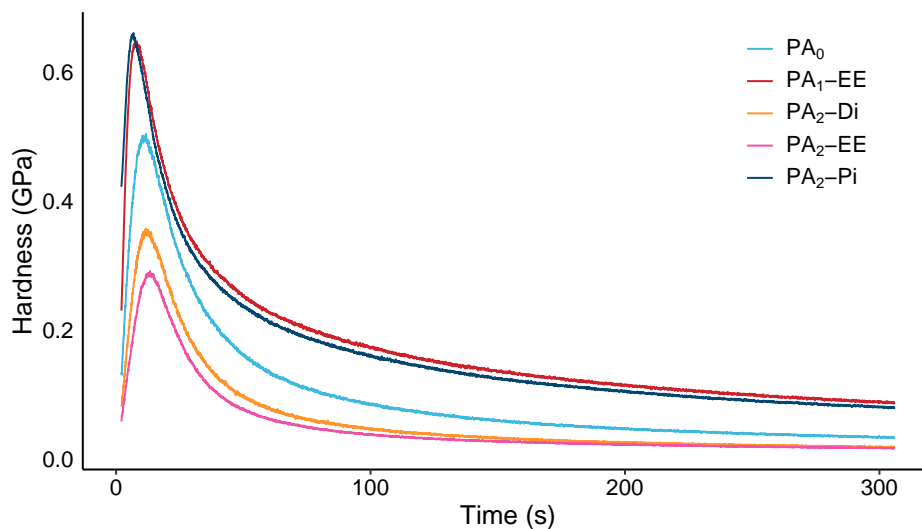


Figure 7: Evolution of hardness versus time during 5 minutes nanoindentation creep test.

of methacrylate-isocyanate monomers and amines were polymerized with MMA and BuA monomers. The self-healing properties of the resulting coatings were afterwards characterized with gloss recovery and optical microscopy. Moreover, the mechanical properties of the coatings showing self-healing properties were measured by nanoindentation creep test. Hardness values were obtained and were in agreement with the  $T_g$  values. Those analyses highlighted the beneficial impact of H-bonds on the self-healing and mechanical properties simultaneously. A polymer based on a MU comonomer synthesized from 2-(2-aminoethoxy)ethanol and 2-isocyanatoethyl methacrylate showed the best self-healing results whilst exhibiting a  $T_g$  value high enough to suit the requirements of protective coatings applications.

The major steps of this work required organic solvents. Due to growing environmental considerations as well as safety and health issues, this project will be adapted for water-based processes. The preparation of the final product would then be closer from the industry requirements.

## Experimental section

### Materials

2-isocyanatoethyl methacrylate and 2-(2-isocyanatoethoxy)ethyl methacrylate were given as free samples from Showa Denko and were used without further purification. Methyl methacrylate (MMA) and *n*-butyl acrylate (BuA) were purchased from Alfa Aesar. The radical inhibitors of those two monomers were preliminary removed through a basic aluminum oxide column. Amines were preliminary distilled if necessary. Diethylamine was purchased from Alfa Aesar and piperidine, *n*-butylamine as well as 2-(2-aminoethoxy)ethanol were purchased from Sigma-Aldrich. Benzoyl peroxide (BPO) was purchased from Fluka. Tetrahydrofuran (THF), hexanes, dichloromethane (DCM) as well as *N,N*-dimethylformamide (DMF) were purchased from Fisher Scientific.

### Apparatus

Nuclear magnetic resonance (NMR) analyses were performed at room temperature on an Agilent DD2 500 MHz spectrometer in deuterated chloroform ( $\text{CDCl}_3$ ). High-resolution mass spectra (HRMS) were obtained with an Agilent 6210 time-of-flight LCMS spectrometer using an ESI ion source. Differential scanning calorimetry (DSC) thermograms were recorded on a Mettler Toledo DSC 823 calorimeter using  $\text{N}_2$  flow with a heating ramp rate of 40 °C/min. Prior to  $T_g$  measurements, the thermal history was erased with a heating scan at 40 °C/min followed by a cooling scan at -5 °C/min. FTIR spectra were carried out using a Bruker Invenio R spectrometer from 350 to 4000  $\text{cm}^{-1}$  with a resolution of 4  $\text{cm}^{-1}$  and 64 scans and using attenuated total reflectance (ATR) mode. Size exclusion chromatography (SEC) analyses were completed at 60 °C with a Variant Instrument PL120 with Styrene-DVB gel column and a DMF eluant containing 20 mM of LiBr with a 1 mL/min flow or with a Tosoh HLC-8321GPC/HT instrument at 80 °C and a Agilent PLgel Mixed-C column (5  $\mu\text{m}$ , 300 x



7.5 mm). In both cases, a refractive index detector was used with a PMMA standard. The gloss of the coatings was measured using a BYK micro-TRI-gloss glossmeter. The values obtained with an angle of 20° were selected. The pictures of the scratches were acquired with a Leica DMRB microscope equipped with a Olympus SC100 camera and their depth was measured with a Bruker Contour GT optical profilometer. Nanoindentation tests were carried out at room temperature on a Bruker TI-Premier dynamic nanoindenter equipped with a Berkovich indenter. Fused quartz was used as a standard reference sample for initial tip calibration. Then, the Bruker's nanoDMA III (nanoscale Dynamic Mechanical Analysis) testing technique was used to perform nanoscale mechanical property measurements. At least 5 indentation creep tests were performed at 80  $\mu\text{N}$  load with superimposing dynamic indentation of 15  $\mu\text{N}$  at a frequency of 200 Hz for 5 minutes. Hardness was calculated according to the Oliver and Pharr model<sup>41</sup>. The Bruker's nanoindenter was also used for in-situ scanning probe microscopy using a 0.5  $\mu\text{N}$  load.

## Synthesis of the monomers

We followed a standard procedure for the synthesis of the MU comonomers (**Scheme 1, Table 1**). For the synthesis of **A<sub>1</sub>-Bu**, **A<sub>1</sub>-Pi**, **A<sub>1</sub>-EE** and **A<sub>2</sub>-Bu**, the appropriate amount of the amine (1 eq.) was dissolved in anhydrous dichloromethane at a concentration of 4.8 M in a dry flask purged under N<sub>2</sub>. The mixture was cooled down to 0 °C and the methacrylate-isocyanate (MI) monomer (1 eq.) was added dropwise. The mixture was stirred overnight, and the solvent was evaporated under vacuum. The product was used without further purification considering a quantitative yield. For **A<sub>1</sub>-Di**, **A<sub>2</sub>-Pi**, **A<sub>2</sub>-Di** and **A<sub>2</sub>-EE**, the synthesis took place in *N,N*-dimethylformamide (DMF) and the solution was directly used as is to avoid undersirable polymerization of the comonomer during solvent evaporation. The success of the MU comonomers synthesis was verified by proton and carbon nuclear magnetic resonance (NMR) of the crude mixture (**Figure S1 to S16** available in Supporting Information) as well as mass spectrometry.

## Synthesis of the polymers and formation of the coatings

MMA (2 eq.), BuA (2 eq.) and BPO (0.1 mol % of the total number of moles of the monomers) were added to the methacrylate-urea (MU) comonomer (1 eq.). Anhydrous DMF was added to suit the desired concentration and the mixture was then degassed under N<sub>2</sub> with three freeze-pump-thaw cycles in liquid N<sub>2</sub>. **PA<sub>1</sub>-Bu**, **PA<sub>1</sub>-Pi**, **PA<sub>1</sub>-Di** and **PA<sub>2</sub>-Bu** were synthesized with a total monomer concentration equal to 4.3 M. It is noteworthy that this concentration had to be lowered for other polymers to avoid an irreversible gelation process. The total monomer concentration for **PA<sub>1</sub>-EE** and **PA<sub>2</sub>-Pi** was then set to 1.5 M and the one for **PA<sub>2</sub>-EE**, **PA<sub>2</sub>-Di** was set to 1 M. The **PA<sub>0</sub>** polymer was prepared with MMA (2.5 eq.) and BuA (2.5 eq.) only, with a concentration of 1 M.

The mixture was heated at 80 °C for 24 hours. The polymerization was quenched by opening the flask to ambient atmosphere and the polymer was precipitated three times in cold water to remove all the DMF. Between each precipitation, it was dissolved in a minimal amount of tetrahydrofuran (THF). The polymer was then precipitated in cold hexanes and dried overnight at 50 °C under vacuum. Hence, the polymers were characterized with <sup>1</sup>H NMR in order to attest the absence of residual monomers and DMF traces. Polymers were then dissolved in THF with a 0.25 g/mL concentration and the solution was deposited on a stainless steel substrate with a thickness of 1 mm. After drying, clear and translucent coatings were formed with thicknesses varying from 30 μm to 100 μm.

## Self-healing tests

The coatings were damaged with an abrasive pad weighted with a 500 g mass. Three linear back and forth were manually made. The coatings were left for one hour to allow them to

spring back and they were then heated in an oven at 75 °C for one hour. Gloss measurements were made prior to the abrasion, after the abrasion and after heating. The gloss recovery (GR) was determined by following **Equation 2** from the gloss value of the virgin sample ( $g_{virgin}$ ), the damaged sample ( $g_{damaged}$ ) and the healed sample ( $g_{healed}$ ).<sup>42</sup>

$$GR = \frac{g_{healed} - g_{damaged}}{g_{virgin} - g_{damaged}} \cdot 100 \quad (2)$$

## Supporting Information

Supporting Information is available from the Wiley Online Library or from the authors.

## Acknowledgements

This work was supported by the Natural Sciences and Engineering Research Council of Canada (NSERC) through the IRC program (Grant No. IRCPJ 514918–16). The authors would like to thank the industrial partners involved in the NSERC-Canlak Industrial Research Chair in Interior Wood Product Finishes : Canlak, Boa-Franc, EMCO-Inortech and Canadel. They also would like to express their gratitude to François Otis, Pierre Audet, Thierry Lefèvre and Yves Bédard for their help with the characterization techniques as well as to Cyril Marsiquet for the nanoindentation tests.

## References

- (1) S. R. White, N. R. Sottos, P. H. Geubelle, J. S. Moore, M. R. Kessler, S. R. Sriram, E. N. Brown, S. Viswanathan, *Nature* **2001**, *409* 794.
- (2) B. J. Blaiszik, N. R. Sottos, S. R. White, *Composites Science and Technology* **2008**, *68*, 3-4 978.

- (3) A. R. Jones, C. A. Watkins, S. R. White, N. R. Sottos, *Polymer* **2015**, *74* 254.
- (4) H. Guo, Y. Han, W. Zhao, J. Yang, L. Zhang, *Nature Communications* **2020**, *11*, 1 1.
- (5) A. Fuhrmann, R. Göstl, R. Wendt, J. Kötteritzsch, M. D. Hager, U. S. Schubert, K. Brademann-Jock, A. F. Thünemann, U. Nöchel, M. Behl, S. Hecht, *Nature Communications* **2016**, *7*.
- (6) K. K. Oehlenschlaeger, J. O. Mueller, J. Brandt, S. Hilf, A. Lederer, M. Wilhelm, R. Graf, M. L. Coote, F. G. Schmidt, C. Barner-Kowollik, *Advanced Materials* **2014**, *26*, 21 3561.
- (7) Y. Lai, X. Kuang, P. Zhu, M. Huang, X. Dong, D. Wang, *Advanced Materials* **2018**, *30*, 38 1.
- (8) J. Canadell, H. Goossens, B. Klumperman, *Macromolecules* **2011**, *44*, 8 2536.
- (9) Z. Deliballi, R. Demir-Cakan, B. Kiskan, Y. Yagci, *Macromolecular Chemistry and Physics* **2022**, 2100423.
- (10) J. J. Cash, T. Kubo, A. P. Bapat, B. S. Sumerlin, *Macromolecules* **2015**, *48*, 7 2098.
- (11) P. Cordier, F. Tournilhac, C. Soulié-Ziakovic, L. Leibler, *Nature* **2008**, *451*, 7181 977.
- (12) A. Faghihnejad, K. E. Feldman, J. Yu, M. V. Tirrell, J. N. Israelachvili, C. J. Hawker, E. J. Kramer, H. Zeng, *Advanced Functional Materials* **2014**, *24*, 16 2322.
- (13) J. H. Xu, J. Y. Chen, Y. N. Zhang, T. Liu, J. J. Fu, *Angewandte Chemie - International Edition* **2021**, *60*, 14 7947.
- (14) Y. Chen, A. M. Kushner, G. A. Williams, Z. Guan, *Nature Chemistry* **2012**, *4*, 6 467.
- (15) D. Mozhdghi, S. Ayala, O. R. Cromwell, Z. Guan, *Journal of the American Chemical Society* **2014**, *136*, 46 16128.

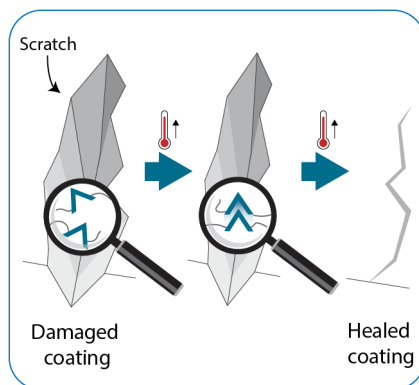
- (16) M. Zhang, F. Zhao, Y. Luo, *ACS Omega* **2019**, *4*, 1 1703.
- (17) S. Burattini, B. W. Greenland, D. H. Merino, W. Weng, J. Seppala, H. M. Colquhoun, W. Hayes, M. E. MacKay, I. W. Hamley, S. J. Rowan, *Journal of the American Chemical Society* **2010**, *132*, 34 12051.
- (18) M. Nakahata, Y. Takashima, A. Harada, *Macromolecular Rapid Communications* **2016**, *37*, 1 86.
- (19) Z. Wang, Y. Ren, Y. Zhu, L. Hao, Y. Chen, G. An, H. Wu, X. Shi, C. Mao, *Angewandte Chemie - International Edition* **2018**, *57*, 29 9008.
- (20) S. J. Kalista, T. C. Ward, *Journal of the Royal Society Interface* **2007**, *4*, 13 405.
- (21) S. J. Kalista, T. C. Ward, Z. Oyetunji, *Mechanics of Advanced Materials and Structures* **2007**, *14*, 5 391.
- (22) A. Das, A. Sallat, F. Böhme, M. Suckow, D. Basu, S. Wießner, K. W. Stöckelhuber, B. Voit, G. Heinrich, *ACS Applied Materials and Interfaces* **2015**, *7*, 37 20623.
- (23) M. W. Urban, D. Davydovich, Y. Yang, T. Demir, Y. Zhang, L. Casabianca, *Science* **2018**, *362* 220.
- (24) R. P. Wool, K. M. O'Connor, *Journal of Applied Physics* **1981**, *52*, 10 5953.
- (25) X. Chen, M. A. Dam, K. Ono, A. Mal, H. Shen, S. R. Nutt, K. Sheran, F. Wudl, *Science* **2002**, *295*, 5560 1698 LP .
- (26) J. Kötteritzsch, R. Geitner, J. Ahner, M. Abend, S. Zechel, J. Vitz, S. Hoepfner, B. Dietzek, M. Schmitt, J. Popp, U. S. Schubert, M. D. Hager, *Journal of Applied Polymer Science* **2018**, *135*, 10 1.
- (27) M. Wouters, E. Craenmehr, K. Tempelaars, H. Fischer, N. Stroeks, J. van Zanten, *Progress in Organic Coatings* **2009**, *64*, 2-3 156.

- (28) J. Kötteritzsch, S. Stumpf, S. Hoepfner, J. Vitz, M. D. Hager, U. S. Schubert, *Macromolecular Chemistry and Physics* **2013**, *214*, 14 1636.
- (29) J. Kötteritzsch, M. D. Hager, U. S. Schubert, *Polymer* **2015**, *69* 321.
- (30) S. Schäfer, G. Kickelbick, *Macromolecules* **2018**, *51*, 15 6099.
- (31) B. Wu, A. Yuan, Y. Xiao, Y. Wang, J. Lei, *Journal of Materials Chemistry C* **2020**, *8*, 36 12638.
- (32) O. Colombani, C. Barioz, L. Bouteiller, C. Chanéac, L. Fompérie, F. Lortie, H. Montés, *Macromolecules* **2005**, *38*, 5 1752.
- (33) J. Courtois, I. Baroudi, N. Nouvel, E. Degrandi, S. Pensec, G. Ducouret, C. Chanéac, L. Bouteiller, C. Creton, *Advanced Functional Materials* **2010**, *20*, 11 1803.
- (34) P. J. Woodward, D. H. Merino, B. W. Greenland, I. W. Hamley, Z. Light, A. T. Slark, W. Hayes, *Macromolecules* **2010**, *43*, 5 2512.
- (35) D. R. Hamann, A. Shukla, P. M. Platzman, E. D. Isaacs, *Physical Review B - Condensed Matter and Materials Physics* **2001**, *64*, 5 1.
- (36) G. Socrates, *Infrared and Raman Characteristic Group Frequencies : Tables and Charts*, John Wiley & Sons Ltd., Chichester, England, 3rd edition, **2004**.
- (37) L. J. Bellamy, *The Infrared Spectra of Complex Molecules*, Chapman and Hall, London, 3rd edition, **1975**.
- (38) F. C. Wang, M. Feve, T. M. Lam, J. Pascault, *Journal of Polymer Science: Part B: Polymer Physics* **1994**, *32*, 8 1315.
- (39) G. C. Pimentel, A. L. McClellan, *The Hydrogen Bond*, W. H. Freeman and Company, London, 1st edition, **1960**.

- (40) L. Chagnon, G. Arnold, S. Giljean, M. Brogly, *Progress in Organic Coatings* **2013**, *76*, 10 1337.
- (41) W. C. Oliver, G. M. Pharr, *Journal of Materials Research* **1992**, *7*, 6 1564.
- (42) B. J. Blaiszik, S. L. B. Kramer, S. C. Olugebefola, J. S. Moore, N. R. Sottos, S. R. White, *Annu. Rev. Mater. Res.* **2011**, *40*, 5 179.

## Table of Contents

In this work, self-healing polyacrylate coatings were prepared using monomers containing urea groups in their side-chains. Those monomers were obtained from easily accessible amines and isocyanates in a one-step synthesis. Self-healing and nanoindentation creep tests highlighted the beneficial impact of H-bonds on the self-healing and mechanical properties simultaneously. A coating showing a complete self-healing after heating 1 hour at 75 °C was successfully obtained.



ToC Entry